Optoelectronic Materials

DOI: 10.1002/ange.201308486

Highly Efficient Near-Infrared Organic Light-Emitting Diode Based on a Butterfly-Shaped Donor–Acceptor Chromophore with Strong Solid-State Fluorescence and a Large Proportion of Radiative Excitons**

Liang Yao, Shitong Zhang, Rong Wang, Weijun Li, Fangzhong Shen, Bing Yang, and Yuguang Ma**

Abstract: *The development of near-infrared (NIR) organic light-emitting diodes (OLEDs) is of growing interest. Donor–acceptor (D–A) chromophores have served as an important class of NIR materials for NIR OLED applications. However, the external quantum efficiencies (EQEs) of NIR OLEDs based on conventional D–A chromophores are typically below 1 %. Reported herein is a butterfly-shaped D–A compound, PTZ-BZP. A PTZ-BZP film displayed strong NIR fluorescence with an emission peak at 700 nm, and the corresponding quantum efficiency reached 16 %. Remarkably, the EQE of the NIR OLED based on PTZ-BZP was 1.54 %, and a low efficiency roll-off was observed, as well as a high radiative exciton ratio of 48 %, which breaks through the limit of 25 % in conventional fluorescent OLEDs. Experimental and theoretical investigations were carried out to understand the excited-state properties of PTZ-BZP.*

Organic light-emitting diodes (OLEDs) that emit visible and white light have found great success in flat-panel displays and solid-state lighting over the past two decades.[1] Extension of the spectrum of OLEDs from visible to deep-red and near-infrared (NIR) has become a new target in the field of OLEDs because of the urgent demand in chemosensing, night-vision devices, and information-secured displays.[2] There have been several types of organic or metal-complex materials utilized for NIR OLEDs, including lanthanide-metal complexes,[3] conjugated polymers,[4] phosphorescent metal complexes,[5] and organic π-conjugated compounds with donor–acceptor (D–A) structures.[6] The external quantum efficiencies (EQEs) of these NIR OLEDs were typically below 1 %. Recently, a significant breakthrough in EQE has been made in NIR phosphorescent OLEDs (POLEDs): An EQE of up to 9.2 % was reported for a platinum(II) porphyrin with extended π-conjugation.[5d] However, these high EQE values of NIR POLEDs usually appeared at very low current densities, and there were serious efficiency roll-offs at high current density and high brightness, probably owing to the long lifetime of triplet excitons in such NIR OLEDs.[7]

The development of metal-free organic materials is of significance, considering their fluorescent nature (avoid quenching of long-lifetime excitons) and cost advantage (without expensive metals). The research is currently focused on π-conjugated compounds with a donor–acceptor (D–A) structure, because a strong D–A interaction could lead to a much narrower band gap, thus resulting in an electronic transition in the deep-red or NIR spectral range.[8] However, these D–A compounds exhibit unexpectedly low efficiency in both photoluminescence and electroluminescence (EL) devices. The main reason for the low efficiency could be ascribed to an intrinsic limitation according to the energy-gap law, which predicts that the quantum efficiency of chromophores decreases as the energy gap is reduced, owing to vibrational overlap of the ground and excited states.[9] Additionally, the HOMO/LUMO overlap in D–A chromophores is usually limited, which always leads to a lower radiative-transition rate, and finally results in virtually no emission.[10] In a solid film, the fluorescence efficiency is further reduced because of the nonradiative process induced by dipole–dipole interactions of these polar chromophores.[11] Thus, for highly efficient NIR OLEDs, the D–A chromophores should possess a reasonable radiative-transition rate, and the fluorescence efficiency should be maintained as well as possible in the solid film. More importantly, further EQE improvement of fluorescent NIR OLEDs (FOLEDs) based on D–A chromophores requires an innovative molecular approach. An increase in the radiative exciton ratio and the use of triplet excitons in FOLEDs may be of great potential, as demonstrated with some D–A compounds reported very recently.[12]

Herein, we report a butterfly-shaped NIR D–A compound, PTZ-BZP (Scheme 1), in which phenothiazine serves as the electron donor and benzothiadiazole as the electron acceptor. The DFT-optimized ground-state geometry (B3LYP/6-31G(d,p) method) reveals that the phenothiazine moiety possesses a nonplanar "butterfly-like" structure with a C-S-N-C dihedral angle (θ_N) of 142°.[13] Furthermore, the phenothiazine and benzothiadiazole groups are twist-linked with a distorted angle (θ_{D-A}) of 145°, which is a relatively planar arrangement for D–A compounds. Generally, the electronic transition of the charge-transfer (CT) excited state is partially forbidden owing to the spatial separation of the donor and acceptor moieties. In our case, in PTZ-BZP, the

[*] L. Yao, S. Zhang, R. Wang, Dr. W. Li, Dr. F. Shen, Prof. B. Yang, Prof. Y. Ma
State Key Laboratory of Supramolecular Structure and Materials
Jilin University
2699 Qianjin Avenue, Changchun, 130012 (P. R. China)
E-mail: yangbing@jlu.edu.cn
ygma@jlu.edu.cn

[**] We are grateful for financial support from the National Science Foundation of China (grant number 91233113, 51273078) and the National Basic Research Program of China (973 Program, grant numbers 2013CB834705 and 2013CB834805).

Supporting information for this article is available on the WWW under http://dx.doi.org/10.1002/anie.201308486.

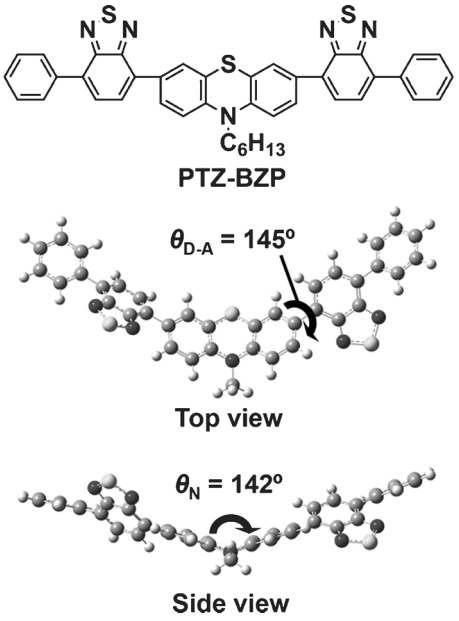

Scheme 1. Molecular structure of PTZ-BZP and DFT-optimized geometry of a simplified structure with a methyl substituent.

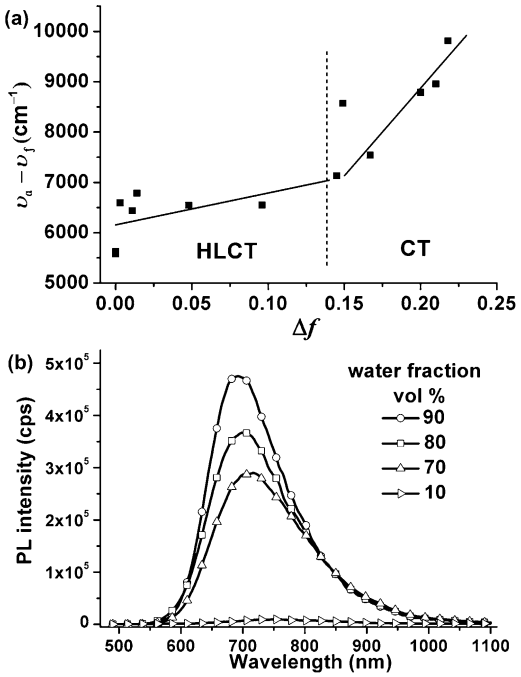

Figure 1. a) Linear correlation of the orientation polarization (Δf) of solvent media with the Stokes shift ($\upsilon_a - \upsilon_f$; a: absorbed light; f: fluorescence) for PTZ-BZP (see Table S1 for the solvents and corresponding data). In low-polarity and high-polarity solvents, the S_1 state is the HLCT state and the CT state, respectively. b) PL spectra of PTZ-BZP (10 μM) in THF/water mixtures with different water fractions.

near-planar arrangement of the phenothiazine and benzothiadiazole groups (θ_{D-A}) may cause considerable orbital overlap between these moieties and further enhance the radiative-transition rate and fluorescence efficiency.

The UV/Vis absorption and photoluminescence (PL) spectra of PTZ-BZP were recorded in various solvents with different polarities (see Figures S4 and S5, respectively, and the detailed data summarized in Table S1 in the Supporting Information). The absorption spectra seldom changed in terms of both their shape and position as the solvent polarity increased, thus implying a rather small dipolar change at the ground state in different solvents. The absorption bands at approximately 447 nm were assigned to the intramolecular CT transition. The fluorescence spectra broadened and revealed a remarkable redshift as the polarity of the solvent increased: from 590 nm in nonpolar hexane to 790 nm in polar dichloromethane. The large solvatochromic shift indicated a strong CT state. The PL quantum yields of PTZ-BZP in different solvents exhibited a clear decreasing trend with increasing solvent polarity: from 0.47 in hexane to 0 in acetonitrile. To better understand the solvent-polarity effect, we applied the Lippert–Mataga relation.[14] Figure 1a shows a plot of the Stokes shift versus the orientation polarizability (Δf). Notably, the plot shows two sets of linearity indicative of two different excited states: one for high-polarity solvents and the other for low-polarity solvents. The dipole moment, μ_e, was calculated to be 31.1 and 13.2 D for high- and low-polarity solvents, respectively. In high-polarity solvents, the μ_e value is larger than that of 4-(*N*,*N*-dimethylamino)benzonitrile (DMABN), which is a typical CT molecule with a μ_e value of 23 D. Furthermore, with increasing solvent polarity, the fluorescence quantum yield rapidly decreased from 0.31 in isopropyl ether to 0.02 in dichloromethane. We concluded that a CT state is dominant in high-polarity solvents. In low-polarity solvents, the dipole moment of 13.2 D indicated that the S_1 state still possessed CT character. Nevertheless, this value was significantly smaller than that in high-polarity solvents. Meanwhile, a relatively high quantum yield (between 0.47 in hexane and 0.32 in butyl ether) could be maintained with increased solvent polarity. These two factors demonstrated that a certain degree of locally excited (LE) character had been introduced. Thus, the S_1 state in low-polarity solvents contained CT and LE components simultaneously. Since single-exponential fluorescence decay was observed for PTZ-BZP in low-polarity solvents, we supposed that a new and unique excited state existed rather than a simple mixture of the LE and CT states. As it combines a large dipole moment and a high radiative-transition rate, we named it the "hybridized local and charge-transfer" (HLCT) state.[15] Very recently, we reported a series of highly luminous D–A compounds based on the "HLCT" state.[15]

In the absorption spectra of the thin film, the compound showed an absorption band at 479 nm, which is significantly red-shifted (by 30 nm) from that in solution, probably as a result of the domination of a more planar D–A conformer in the aggregated state. In the PL spectrum of the film, PTZ-BZP exhibited a broad emission ranging from 600 to 1000 nm with a peak at 700 nm, thus covering the NIR region well. The Stokes shift of 6591 cm^{-1} lies between that of butyl ether (6549 cm^{-1}) and that of isopropyl ether (7132 cm^{-1}). The results indicate that the polarity of the PTZ-BZP film was similar to that of a low-polarity solvent, and that the S_1 state of the PTZ-BZP film was also a HLCT state. A remarkable quantum efficiency of 16% was observed for the neat film. To

investigate the influence of aggregation effects on the fluorescence behavior, we measured the PL spectra of PTZ-BZP in THF/water mixtures with different water fractions (f_w; Figure 1b), which enabled direct tuning of the solvent polarity and the extent of solute aggregation. The solutions with $f_w \leq 60$ vol% were nearly non-emissive, and the PL curve was practically a flat line parallel to the x axis, mainly as a result of the CT effect induced by the strong polarity of the THF/water mixtures. Fluorescence appeared from $f_w \approx 70$ vol% and was enhanced by further increases in f_w. Evidently, PTZ-BZP is aggregation-induced-emission (AIE) active.[16] The main reason for the AIE phenomenon could be that the HLCT state in the aggregated state is associated with a more efficient radiative electron transition than the CT state in solutions in THF. Therefore, the HLCT state provides a novel approach for the design of highly luminous D–A chromophores. On the other hand, the formation of intermolecular aggregates tends to restrict the rotation described by θ_N and θ_{D-A}, and avoids the nonradiative decay channel, which enhances fluorescence efficiency.[16]

To verify the high potential of PTZ-BZP as a light-emission material for use in optoelectronic devices, we fabricated an undoped NIR OLED with the configuration: ITO/PEDOT:PSS (40 nm)/NPB (80 nm)/TCTA (5 nm)/PTZ-BZP (30 nm)/TPBi (30 nm)/LiF (0.5 nm)/Al (120 nm; ITO = indium tin oxide, PEDOT = poly(3,4-ethylenedioxythiophene), PSS = poly(styrene sulfonate), NPB = *N*,*N*′-bis(naphthalen-1-yl)-*N*,*N*′-bis(phenyl)benzidine, TCTA = tris(4-carbazoyl-9-ylphenyl)amine, TPBi = 1,3,5-tris(1-phenyl-1*H*-benzimidazol-2-yl)benzene. As shown in Figure 2, the EL spectrum of the PTZ-BZP device was almost identical to the PL spectrum of the evaporated film. Although our instrument (PR-650 Spectroscan spectrometer) could not detect the EL luminance signal over 780 nm, it can be inferred that the EL spectrum was extended to nearly 1000 nm according to the PL spectrum of the PTZ-BZP film. Additionally, the EL spectrum showed little change under different driving voltages, thus indicating that the PTZ-BZP device possesses excellent spectral stability. A maximum EQE of 1.54% and brightness of 780 cd m^{-2} were observed for the nondoped NIR OLED based on PTZ-BZP. At a high current density of 300 mA cm^{-2}, the EQE of the PTZ-BZP device still remained as high as 1.17%, which is indicative of a relatively low efficiency roll-off. To the best of our knowledge, the performance of the PTZ-BZP device places it among the best undoped NIR FOLEDs.[6,8,11]

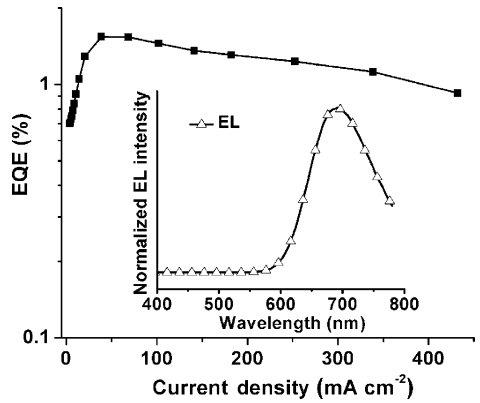

Figure 2. EQE–current-density characteristics of the device. The inset graph is the EL spectrum.

The theoretical value of the radiative exciton ratio was calculated by the following equation:

$$\eta_{ext} = \gamma\,\eta_r\,\eta_{PL}\,\eta_{out} \quad (1)$$

in which η_r is the radiative exciton ratio, η_{ext} is the external quantum efficiency, η_{out} is the light out-coupling efficiency (ca. 20%), η_{PL} is the intrinsic photoluminescence efficiency (ca. 16%), and γ is the recombination efficiency of injected holes and electrons, which is ideally 100% only if holes and electrons are fully balanced and completely recombined to form excitons. Thus, the η_r value of the PTZ-BZP device was calculated to be 48%, which breaks through the limit of the radiative exciton ratio of 25% for conventional FOLEDs. Since no delayed fluorescence was observed from transient PL, and the luminance of EL displayed a linear increase with increasing current density, the high radiative exciton ratio does not seem to be in accordance with some mainstream views, such as thermally activated delayed fluorescence (TADF)[12] or triplet–triplet annihilation (TTA).[17]

To explain the high radiative exciton ratio in the PTZ-BZP device, we calculated and analyzed the energy landscape and the natural transition orbitals (NTOs) of the singlet and triplet states on the basis of TDDFT results with M06-2X/6-31G(d,p) (Figure 3). For the S_1 state, the hole and particle NTOs showed an excellent balance between spatial separation and orbital overlap. The well-separated orbitals led to CT character with a large dipole moment. On the other hand, certain orbital overlaps induced LE character and ensured a reasonable radiative-transition rate. The calculated results demonstrate the coexistence of CT and LE components, in good agreement with our definition of the HLCT state. The low-lying triplet state T_1 was a LE state, and its hole and particle were almost completely overlapped. The energy gap between the S_1 state and the T_1 state reached 0.79 eV, and correspondingly, reverse intersystem crossing (RISC) from the T_1 state to the S_1 state by TADF is not a facile process. The T_2 and T_1 states are degenerate states. The high-lying triplet excited state T_3 (referred to herein as a "hot" excited state) was found to be a HLCT state whose configuration is quite similar to that of the S_1 state. As shown in Figure 3, the energy levels of the S_1 state (2.91 eV) and the T_3 state (2.92 eV) are almost identical. Such small singlet–triplet splitting could offer a potential RISC $T_3 \rightarrow S_1$ process, which we refer to as a "hot-exciton" process.[18] On the other hand, the energy gap between the T_3 state and the T_2 or T_1 state is 0.76 eV. According to the energy-gap law, the internal-conversion (IC) rate, $k_{IC(T)}$, from the T_3 state to the T_2 state may be lower than the RISC rate, k_{RISC}, from the T_3 to the S_1 state.[19] Besides, it has been reported that the RISC rate can be greatly enhanced in some heterocyclic systems with sulfur atoms owing to improved spin–orbit coupling.[20] Therefore, when triplet excitons relax to the lowest vibrational level of T_1, a fraction of them may be converted into singlet excitons through the $T_3 \rightarrow S_1$ channel. Since the concentration of triplet excitons is

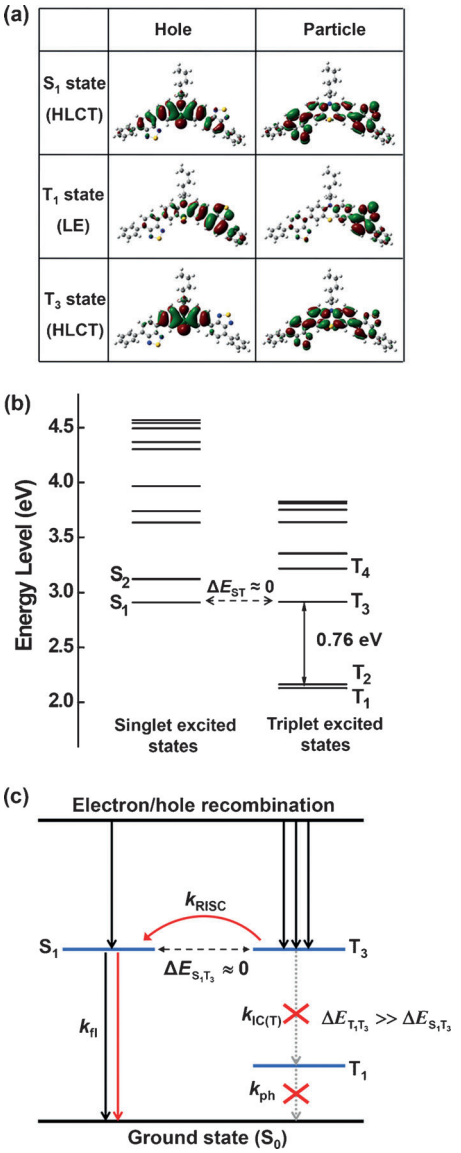

Figure 3. a) Natural transition orbitals for S_1, T_1, and T_3. b) The energy landscape for singlet and triplet excited states. c) Model for exciton relaxation in the EL process. RISC: reverse intersystem crossing; IC(T): internal conversion between the triplet states; fl: fluorescence; ph: phosphorescence.

much higher than that of singlet excitons, the dynamic equilibrium will promote the conversion from triplet excitons into singlet excitons in the electroluminescence process. We deduce that the efficient RISC provided by the hot-exciton process is responsible for the radiative exciton ratio of over 25% in the PTZ-BZP device.

In summary, we have investigated the optoelectronic properties of an NIR D–A compound, PTZ-BZP. Photophysical and DFT analysis demonstrated that the S_1 state of PTZ-BZP in low-polarity solvent and as a thin film shows HLCT character. It benefits from the large dipole moment of the CT state and a certain degree of orbital overlap of the LE state, thus making the compound a potentially highly luminous molecule. In the aggregated state, PTZ-BZP displays strong NIR emission and AIE behavior. The EQE of the undoped PTZ-BZP device is 1.54%: among the highest observed for undoped NIR FOLEDs. Notably, in the device, a high radiative exciton ratio of 48% was observed, which exceeds the limit of 25% in conventional FOLEDs, probably as a result of efficient RISC through the hot-exciton process. Therefore, PTZ-BZP could serve as an attractive light-emitting material in NIR OLEDs, and our study should provide new ideas for the design of efficient NIR-fluorescent molecules by emphasizing the full use of both singlet and triplet excitons.

Received: September 29, 2013
Revised: December 15, 2013
Published online: January 21, 2014

Keywords: chromophores · donor–acceptor systems · near-infrared fluorescence · optoelectronic materials · organic light-emitting diodes

[1] a) M. A. Baldo, D. F. O'Brien, Y. You, A. Shoustikov, S. Sibley, M. E. Thompson, S. R. Forrest, *Nature* **1998**, *395*, 151–154; b) Y. Sun, N. C. Giebink, H. Kanno, B. Ma, M. E. Thompson, S. R. Forrest, *Nature* **2006**, *440*, 908–912; c) A. C. Grimsdale, K. L. Chan, R. E. Martin, P. G. Jokisz, A. B. Holmes, *Chem. Rev.* **2009**, *109*, 897–1091; d) Q. Wang, D. Ma, *Chem. Soc. Rev.* **2010**, *39*, 2387–2398.

[2] a) G. Qian, Z. Y. Wang, *Chem. Asian J.* **2010**, *5*, 1006–1029; b) N. Tessler, V. Medvedev, M. Kazes, S. Kan, U. Banin, *Science* **2002**, *295*, 1506–1508; c) B. Stender, S. F. Völker, C. Lambert, J. Pflaum, *Adv. Mater.* **2013**, *25*, 2943–2947; d) W. Qin, D. Ding, J. Liu, W. Zhang Yuan, Y. Hu, B. Liu, B. Z. Tang, *Adv. Funct. Mater.* **2012**, *22*, 771–779.

[3] a) J. Kido, *Chem. Rev.* **2002**, *102*, 2357–2368; b) R. G. Sun, Y. Z. Wang, Q. B. Zheng, H. J. Zhang, A. J. Epstein, *J. Appl. Phys.* **2000**, *87*, 7589–7591.

[4] a) T. T. Steckler, O. Fenwick, T. Lockwood, M. R. Andersson, F. Cacialli, *Macromol. Rapid Commun.* **2013**, *34*, 990–996; b) B. C. Thompson, L. G. Madrigal, M. R. Pinto, T.-S. Kang, K. S. Schanze, J. R. Reynolds, *J. Polym. Sci. Part A* **2005**, *43*, 1417–1431; c) M. Sun, X. Jiang, W. Liu, T. Zhu, F. Huang, Y. Cao, *Synth. Met.* **2012**, *162*, 1406–1410.

[5] a) C. Borek, K. Hanson, P. I. Djurovich, M. E. Thompson, K. Aznavour, R. Bau, Y. R. Sun, S. R. Forrest, J. Brooks, L. Michalski, J. Brown, *Angew. Chem.* **2007**, *119*, 1127–1130; *Angew. Chem. Int. Ed.* **2007**, *46*, 1109–1112; b) H. Xiang, J. Cheng, X. Ma, X. Zhou, J. J. Chruma, *Chem. Soc. Rev.* **2013**, *42*, 6128–6185; c) O. Fenwick, J. K. Sprafke, J. Binas, D. V. Kondratuk, F. Di Stasio, H. L. Anderson, F. Cacialli, *Nano Lett.* **2011**, *11*, 2451–2456; d) K. R. Graham, Y. Yang, J. R. Sommer, A. H. Shelton, K. S. Schanze, J. Xue, J. R. Reynolds, *Chem. Mater.* **2011**, *23*, 5305–5312.

[6] a) G. Qian, Z. Zhong, M. Luo, D. Yu, Z. Zhang, Z. Y. Wang, D. Ma, *Adv. Mater.* **2009**, *21*, 111–116; b) G. Qian, B. Dai, M. Luo, D. Yu, J. Zhan, Z. Zhang, D. Ma, Z. Y. Wang, *Chem. Mater.* **2008**, *20*, 6208–6216; c) G. Qian, Z. Zhong, M. Luo, D. Yu, Z. Zhang, D. Ma, Z. Y. Wang, *J. Phys. Chem. C* **2009**, *113*, 1589–1595; d) Y. Yang, R. T. Farley, T. T. Steckler, S. H. Eom, J. R. Reynolds, K. S. Schanze, J. Xue, *J. Appl. Phys.* **2009**, *106*, 044509.

[7] a) N. C. Giebink, S. R. Forrest, *Phys. Rev. B* **2008**, *77*, 235215; b) W. Staroske, M. Pfeiffer, K. Leo, M. Hoffmann, *Phys. Rev. Lett.* **2007**, *98*, 197402.

[8] a) S. Ellinger, K. R. Graham, P. Shi, R. T. Farley, T. T. Steckler, R. N. Brookins, P. Taranekar, J. Mei, L. A. Padilha, T. R. Ensley, H. Hu, S. Webster, D. J. Hagan, E. W. V. Stryland, K. S. Schanze,

J. R. Reynolds, *Chem. Mater.* **2011**, *23*, 3805 – 3817; b) X. Du, J. Qi, Z. Zhang, D. Ma, Z. Y. Wang, *Chem. Mater.* **2012**, *24*, 2178 – 2185.

[9] a) J. V. Caspar, E. M. Kober, B. P. Sullivan, T. J. Meyer, *J. Am. Chem. Soc.* **1982**, *104*, 630 – 632; b) S. D. Cummings, R. Eisenberg, *J. Am. Chem. Soc.* **1996**, *118*, 1949 – 1960.

[10] M. Van der Auweraer, Z. R. Grabowski, W. Rettig, *J. Phys. Chem.* **1991**, *95*, 2083 – 2092.

[11] M. Shimizu, R. Kaki, Y. Takeda, T. Hiyama, N. Nagai, H. Yamagishi, H. Furutani, *Angew. Chem.* **2012**, *124*, 4171 – 4175; *Angew. Chem. Int. Ed.* **2012**, *51*, 4095 – 4099.

[12] a) H. Uoyama, K. Goushi, K. Shizu, H. Nomura, C. Adachi, *Nature* **2012**, *492*, 234 – 238; b) G. Méhes, H. Nomura, Q. Zhang, T. Nakagawa, C. Adachi, *Angew. Chem.* **2012**, *124*, 11473 – 11477; *Angew. Chem. Int. Ed.* **2012**, *51*, 11311 – 11315; c) Q. Zhang, J. Li, K. Shizu, S. Huang, S. Hirata, H. Miyazaki, C. Adachi, *J. Am. Chem. Soc.* **2012**, *134*, 14706 – 14709; d) J. Li, T. Nakagawa, Q. Zhang, H. Nomura, H. Miyazaki, C. Adachi, *Adv. Mater.* **2013**, *25*, 3319 – 3323.

[13] a) L. Yao, S. Sun, S. Xue, S. Zhang, X. Wu, H. Zhang, Y. Pan, C. Gu, F. Li, Y. Ma, *J. Phys. Chem. C* **2013**, *117*, 14189 – 14196; b) G. Kim, H. R. Yeom, S. Cho, J. H. Seo, J. Y. Kim, C. Yang, *Macromolecules* **2012**, *45*, 1847 – 1857.

[14] a) V. E. Z. Lippert, *Electrochemistry* **1957**, *61*, 962 – 975; b) N. Mataga, Y. Kaifu, M. Koizumi, *Bull. Chem. Soc. Jpn.* **1956**, *29*, 465 – 470.

[15] a) W. Li, D. Liu, F. Shen, D. Ma, Z. Wang, T. Feng, Y. Xu, B. Yang, Y. Ma, *Adv. Funct. Mater.* **2012**, *22*, 2797 – 2803; b) S. Tang, W. Li, F. Shen, D. Liu, B. Yang, Y. Ma, *J. Mater. Chem.* **2012**, *22*, 4401 – 4408; c) W. Li, Y. Pan, R. Xiao, Q. Peng, S. Zhang, D. Ma, F. Li, F. Shen, Y. Wang, B. Yang, Y. Ma, *Adv. Funct. Mater.* **2013**, DOI: 10.1002/adfm.201301750; d) S. Zhang, W. Li, L. Yao, Y. Pan, F. Shen, R. Xiao, B. Yang, Y. Ma, *Chem. Commun.* **2013**, *49*, 11302 – 11304.

[16] a) X. Y. Shen, W. Z. Yuan, Y. Liu, Q. Zhao, P. Lu, Y. Ma, I. D. Williams, A. Qin, J. Z. Sun, B. Z. Tang, *J. Phys. Chem. C* **2012**, *116*, 10541 – 10547; b) C. Y. K. Chan, Z. Zhao, J. W. Y. Lam, J. Liu, S. Chen, P. Lu, F. Mahtab, X. Chen, H. H. Y. Sung, H. S. Kwok, Y. Ma, I. D. Williams, K. S. Wong, B. Z. Tang, *Adv. Funct. Mater.* **2012**, *22*, 378 – 389; c) Y. P. Li, F. Li, H. Y. Zhang, Z. Q. Xie, W. J. Xie, H. Xu, B. Li, F. Shen, L. Ye, M. Hanif, D. Ma, Y. Ma, *Chem. Commun.* **2007**, 231 – 233.

[17] a) C.-J. Chiang, A. Kimyonok, M. K. Etherington, G. C. Griffiths, V. Jankus, F. Turksoy, A. P. Monkman, *Adv. Funct. Mater.* **2013**, *23*, 739 – 746; b) D. Y. Kondakov, T. D. Pawlik, T. K. Hatwar, J. P. Spindler, *J. Appl. Phys.* **2009**, *106*, 124510.

[18] a) J. Guo, H. Ohkita, H. Benten, S. Ito, *J. Am. Chem. Soc.* **2009**, *131*, 16869 – 16880; b) J. Lee, K. Vandewal, S. R. Yost, M. E. Bahlke, L. Goris, M. A. Baldo, J. V. Manca, T. V. Voorhis, *J. Am. Chem. Soc.* **2010**, *132*, 11878 – 11880.

[19] N. J. Turro, *Modern Molecular Photochemistry*, University Science Books, Sausalito, **1991**, pp. 148 – 149.

[20] a) W. Barford, *Phys. Rev. B* **2004**, *70*, 205204; b) G. Cui, W.-h. Fang, *J. Chem. Phys.* **2013**, *138*, 044315.

